scientific reports

Check for updates

OPEN

Determination of hydrocortisone and cortisone in artificial saliva by spray assisted fine droplet formation liquid phase microextraction coupled to LC–MS/MS

Selim Gürsoy[1,2], Süleyman Bodur[3,4,5], Arda Atakol[6] & Sezgin Bakırdere[3,7]✉

Hydrocortisone and cortisone are clinically informative steroids whose joint measurement at low concentrations is essential for ratio-reliable interpretation. A spraying-assisted fine droplet formation liquid-phase microextraction (SA-FDF-LPME) was combined with liquid chromatography–tandem mass spectrometry (LC–MS/MS) for simultaneous quantitation in saliva-type matrices as part of a method-development study. Method parameters were optimized to secure chromatographic resolution, stable ion ratios, and high sensitivity. Under direct injection, LOD/LOQ values were 1.05/3.50 µg kg^{-1} for cortisone and 0.80/2.68 µg kg^{-1} for hydrocortisone, with dynamic ranges of 3.65–150.77 and 2.59–268.45 µg kg^{-1}, respectively. With SA-FDF-LPME coupled to LC–MS/MS, LOD/LOQ were 0.0164/0.0547 µg kg^{-1} for cortisone and 0.0734/0.245 µg kg^{-1} for hydrocortisone, and dynamic ranges were 0.049–4.983 and 0.210–5.50 µg kg^{-1}, respectively. Accuracy was established by pre-extraction spiking at different concentrations in two artificial saliva formulations. Using external-standard calibration, recoveries were 105.3–129.4%/110.4–141.1% for cortisone and 110.0–134.9%/94.1–142.8% for hydrocortisone; with matrix-matched calibration, recoveries were 80.3–103.2%/98.1–117.8% for cortisone and 79.8–105.7%/97.3–114.0% for hydrocortisone. The developed SA-FDF-LPME–LC–MS/MS method enables sensitive, accurate, and simultaneous quantification of hydrocortisone and cortisone at saliva-relevant concentrations and offers a practical platform for selective bioanalysis of related small molecules.

Keywords Artificial saliva, Hydrocortisone, Cortisone, Spraying assisted fine droplet formation liquid phase microextraction, Tandem mass spectrometry

Glucocorticoids regulate the human stress response, intermediary metabolism, immune function, and circadian physiology[1,2]. Hydrocortisone (cortisol) is the bioactive hormone, and cortisone is its oxidized counterpart[3]. Interconversion by tissue-specific 11β-hydroxysteroid dehydrogenase isoenzymes (11β-HSD) sets local glucocorticoid tone, with 11β-HSD1 primarily catalyzing the regeneration of hydrocortisone from cortisone in metabolic tissues and 11β-HSD2 predominantly catalyzing the inactivation of hydrocortisone to cortisone in mineralocorticoid target tissues[4–6]. Deficiency of 11β-HSD2 is associated with the syndrome of apparent mineralocorticoid excess[7]. Hydrocortisone exerts broad clinical effects across immune, cardiovascular, and homeostatic systems and has central roles in metabolic regulation[2,3]. Developmental context is pertinent, as

[1]Deparment of Analytical Chemistry School of Pharmacy, İstanbul Medipol University, 34810 Istanbul, Turkey. [2]Department of Bioengineering, Yıldız Technical University, 34220 Istanbul, Turkey. [3]Faculty of Art and Science Department of Chemistry, Yıldız Technical University, 34220 Istanbul, Turkey. [4]Faculty of Pharmacy Department of Analytical Chemistry, İstinye University, 34010 Istanbul, Turkey. [5]Scientific and Technological Research Application and Research Center, İstinye University, 34010 Istanbul, Turkey. [6]Faculty of Pharmacy Department of Analytical Chemistry, Kent University, 34406 Istanbul, Turkey. [7]Turkish Academy of Sciences (TÜBA), Vedat Dalokay Street, No: 112, 06670, 06690 Çankaya, Ankara, Turkey. ✉email: bsezgin23@yahoo.com

cortisone is more prevalent than hydrocortisone in fetomaternal tissues, and its concentration declines rapidly after birth[8]. The concentrations of hydrocortisone and cortisone, along with their relative ratio, are essential for the diagnosis and management of adrenal insufficiency and hypercortisolism. They are also key in identifying 11β-HSD dysfunction, including apparent mineralocorticoid excess; assessing tissue-level glucocorticoid activation linked to cardiometabolic risk; guiding hydrocortisone replacement therapy; and evaluating drug-enzyme interactions and other exogenous modulators[9–11]. In practice, measurements are required across multiple matrices, including serum or plasma, urine, and saliva, each imposing distinct constraints on selectivity, sensitivity, and robustness, causing specific challenges for analysis[12]. In serum or plasma, abundant proteins and phospholipids can strongly influence electrospray ionization during LC–MS/MS analysis, necessitating highly effective cleanup. In urine, extraction and partitioning are altered by variable ionic strength and urea content. In saliva, low endogenous concentrations, mucins, and pronounced diurnal variation have a poor impact on the detection limits[12–14]. Reported salivary concentrations of hydrocortisone and cortisone are typically in the low μg L^{-1} (ng mL^{-1}) range, with late-night reference intervals for hydrocortisone of roughly 0.2–1.0 μg L^{-1} and corresponding cortisone concentrations often around 1–5 μg L^{-1}, and higher values observed at awakening and in hypercortisolemic states; these small absolute concentrations, combined with matrix viscosity and organic content, underline the need for sample-preparation strategies that condition the saliva matrix and improve overall analysis sensitivity[15].

Meeting those demands requires control of interference and matrix effects. Hydrocortisone and cortisone are structural near-isomers with similar polarity and are likely to co-elute or generate overlapping fragments[16,17]. Insufficient separation or cleanup can bias the hydrocortisone-to-cortisone ratio and undermine clinical interpretation[18]. In response to these constraints, immunoassays have been applied for throughput but are affected by cross-reactivity and calibration drift, while gas chromatography-mass spectrometry offers strong selectivity at the expense of derivatization and extended handling[19,20]. Liquid chromatography-tandem mass spectrometry has been adopted widely because structural specificity and sub-ng mL^{-1} sensitivity can be achieved without derivatization, provided that baseline chromatographic separation is secured and that sample preparation yields clean, preconcentrated extracts with minimal matrix effect. For this reason, coupling with liquid-phase microextraction (LPME) has been favored[21,22].

Within liquid-phase microextraction, formats such as dispersive liquid–liquid microextraction (DLLME), hollow-fiber LPME, and single-drop microextraction have been established[23]. Although solvent use is reduced and mass transfer is accelerated, these approaches can still rely on relatively high disperser volumes, show sensitivity to emulsion stability in protein-rich media, require delicate handling or dedicated consumables, and introduce variability when dispersion or drop formation is performed manually[23,24]. To address these limitations while retaining compatibility with the LC–MS/MS, spray assisted fine droplet formation liquid phase microextraction (SA-FDF-LPME) is employed. A propellant-free nasal atomizer aerosolizes a premixed disperser-extractant directly into the prepared sample and generates a dense field of microdroplets with a transient emulsion. Interfacial area is increased, mass transfer is shortened to seconds, dose-to-dose reproducibility is improved through metered actuation, and the total solvent burden is reduced relative to traditional dispersion or fiber-based setups[25].

In this study, an SA-FDF-LPME-LC–MS/MS method was developed for the simultaneous and ratio-reliable determination of hydrocortisone and cortisone across relevant biofluids, with a focus on saliva-type matrices. Two artificial saliva formulations were employed as matrix surrogates to represent real saliva during recovery experiments, enabling systematic assessment of matrix effects under controlled yet saliva-like conditions. Accordingly, all experiments were conducted using artificial saliva matrices as part of a method-development framework, while chromatographic and mass-spectrometric parameters were optimized to achieve a baseline separation and a robust identification, while the SA-FDF-LPME variables were tuned to maximize enrichment and minimize matrix effects, and linearity, sensitivity, accuracy, repeatability, recovery, and matrix-effect characteristics were established alongside an assessment and practical throughput.

Materials and methods

Standards and chemicals

Hydrocortisone (H4001, ≥98%, Sigma-Aldrich, St. Louis, MO, USA; CAS 50-23-7) and cortisone (C2755, ≥95%, Sigma-Aldrich, St. Louis, MO, USA; CAS 53-06-5) were used as analytical standards. Solution preparation and dilution operations were performed gravimetrically by using an analytical balance. Primary stock solutions were prepared in HPLC-grade methanol (MeOH) at 1008.62 mg kg^{-1} (hydrocortisone) and 932.70 mg kg^{-1} (cortisone). The working solutions for calibration and spiking experiments were obtained by serial dilution with appropriate additions of MeOH and water to obtain matching MeOH concentrations. LC–MS grade MeOH, acetonitrile (ACN), and formic acid were purchased from Merck (Darmstadt, Germany). The extraction solvents used for SA-FDF-LPME were chloroform (≥99.0%), 1,2-dichloroethane (≥99.5%), and dichloromethane (≥99.9%) (Merck, Darmstadt, Germany). Ultrapure water was produced by a Human Power I purification system (resistivity ≥18.3 MΩ·cm). All standards and working solutions were stored in amber glass at 4 °C and equilibrated to room temperature prior to analysis. The preparation of the artificial saliva formulations is described in the subsection "Preparation of artificial saliva and samples".

Instrumentation

Chromatographic separation, detection, and quantitation were performed on a Shimadzu LC2010A HT high-performance liquid chromatography (HPLC) system (Kyoto, Japan) hyphenated to an AB SCIEX 3200 atmospheric-pressure ionization triple-quadrupole mass spectrometer (API-MS/MS, Framingham, USA). Electrospray ionization in the positive mode was applied for obtaining the related precursor and product ions belonging to cortisone and hydrocortisone. Nitrogen for nebulization, curtain, and collision gases was supplied

by a Peak Scientific Genius NM32LA nitrogen generator (Inchinnan, UK). Centrifugation during sample preparation and phase separation was conducted using a Hitachi CT15E benchtop centrifuge and an Eppendorf 5810 centrifuge equipped with a fixed-angle rotor. A propellant-free nasal atomizer was employed for spray-assisted fine-droplet formation LPME. Data acquisition and processing were carried out using Analyst 1.6.2 software (AB SCIEX).

Preparation of artificial saliva and samples

Two artificial saliva formulations (detailed in supplementary Table S1) were prepared by slightly modifying the literature information[26,27]. Reagents were weighed on a four-decimal analytical balance, dissolved sequentially in ultrapure water under magnetic stirring at ambient temperature, mixed for 30 min, and pH was set to 6.8–7.0.8.0 with 0.10 mol L^{-1} HCl or NaOH. The formulations were used as matrix surrogates to reflect the ionic strength and organic load of human saliva, stored at 4 °C for ≤ 48 h, and equilibrated to room temperature prior to analysis. In the present study, artificial saliva was intentionally selected as the experimental matrix to support method development under controlled and well-defined conditions, without introducing the ethical constraints and inter-individual variability inherent to clinical saliva samples.

To replicate the sample-conditioning workflow for native saliva, a methanol-induced protein/mucin precipitation step was implemented prior to the SA-FDF-LPME while maintaining a constant solvent fraction[28]. Artificial saliva (1.20 g) was weighed into polypropylene tubes, spiked with methanolic working solutions of hydrocortisone and cortisone to the targeted concentrations, and the total mass was brought to 2.00 g with MeOH. Gravimetric handling was chosen at this stage because native saliva is a viscous, protein- and mucin-rich fluid prone to foaming and incomplete drainage from volumetric glassware; treating the artificial formulations analogously minimizes volume-related errors, and after dilution to 33.0 g the conditioned solution can be regarded as having an approximate density of 1.0 g mL^{-1} for subsequent volumetric steps. After vortex-mixing for 30 **s**, samples were centrifuged at 12,857 *xg* for 10 min at room temperature. The clarified supernatant (1.83 g) was transferred to a clean tube and diluted to 33.0 g with distilled water to obtain the matrix-matched working solution used for the SA-FDF-LPME. This conditioning mirrored real-saliva handling, reduced viscosity, removed precipitable proteins and mucinous material, and standardized solvent strength across the calibration range.

Accordingly, while the described procedure is suitable for method development and analytical performance characterization in artificial saliva, extension to quantitative analysis in native human saliva would require further studies in real biological matrices, together with full bioanalytical validation in accordance with ICH M10, before application for clinical purposes can be considered.

SA-FDF-LPME procedure

A sample or standard solution of 8.0 mL was transferred into a polypropylene centrifuge tube, and the tube was coupled to the spray apparatus described in our previous studies[25,29]. The extractant was introduced in three consecutive actuations of the spraying apparatus to ensure a fine aerosol of dichloromethane dispersed across the aqueous phase and generated a transient microdroplet field. The dispersion step established a very high interfacial area, and mass transfer into the organic phase proceeded rapidly.

Phase disengagement was promoted by centrifugation at 12,857 *xg* for 1.0 min immediately after vortexing for 15 s. The organic layer enriched in analytes was recovered quantitatively with an automated micropipette and transferred to a clean microcentrifuge tube. The solvent was removed to dryness using a vacuum oven set at 30 °C to limit thermal stress and ensure the complete elimination of any residual extractant. The dry residue was then reconstituted with 50 µL of methanol, and the solution was mixed for 10 s on a vortex mixer until full dissolution was achieved. The resulting solution was directly introduced into the LC–MS/MS system for quantification.

Operational controls included inspection and cleaning of the spray nozzle between extractions to maintain actuation reproducibility, avoidance of prolonged contact between the organic phase and plasticized surfaces, and routine blank extractions to monitor for carryover. Repeatability was assessed by performing SA-FDF-LPME and LC–MS/MS analysis in replicate ($n = 3$ during method optimisation and $n = 6$ for calibration methods), and precision was expressed as the relative standard deviation (%RSD) of the measured concentrations. A schematic representation of the workflow is provided in Fig. 1.

Performance of the sample preparation method

Method performance was evaluated for linearity, detection capability, and recovery using two systems, namely LC–MS/MS alone and SA-FDF-LPME coupled to LC–MS/MS. Calibration graphs were obtained by plotting peak area against concentration, and separate calibration ranges were established for each system to reflect their different sensitivity. Linearity across the working ranges was confirmed by a coefficient of determination near unity, along with satisfactory agreement between back-calculated and nominal concentrations.

Limits of detection (LOD) and limit of quantification (LOQ) were established for both systems to demonstrate the sensitivity gain afforded by microextraction. LOD was defined as the lowest level giving a signal-to-noise ratio of at least three on the quantifier transition, and LOQ as the lowest level giving a ratio of at least ten under the corresponding preparation and acquisition conditions. In addition, concentration-based estimates were calculated from the calibration data using the relations $LOD = 3\sigma/m$ and $LOQ = 10\sigma/m$, where σ denotes the standard deviation of the lowest concentration under the full workflow and m denotes the slope of the calibration graph generated under the same method. Method accuracy was examined in two distinct artificial saliva matrices by pre-extraction spiking at various concentration levels spanning along the calibration range for each matrix, followed by the complete preparation and analysis sequence. Percent recovery at each level was

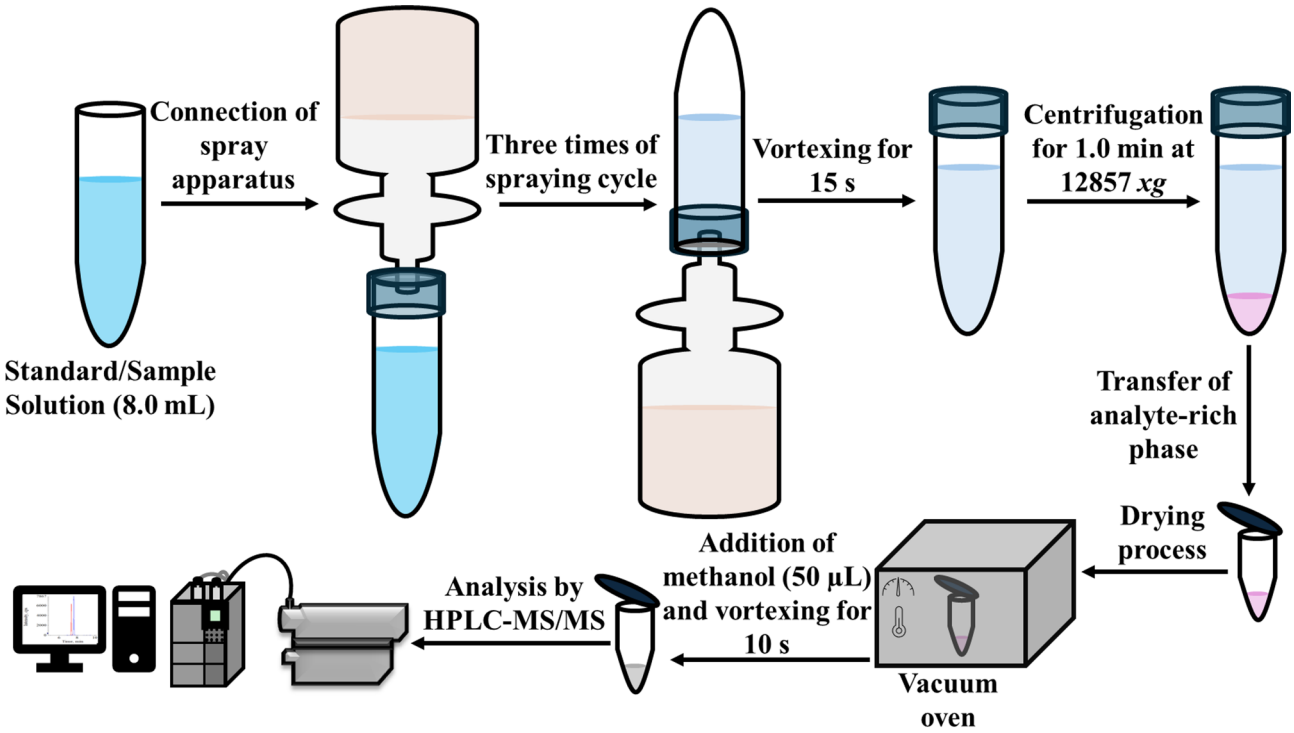

Fig. 1. Flow diagram of SA-FDF-LPME followed by LC–MS/MS analysis.

Analyte	Precursor m/z (Q1)	Product m/z (Q3)	DP (V)	EP (V)	CEP (V)	CE (eV)	CXP (V)
Hydrocortisone	363.6	121.0	30	9	18	33	3
		327.0	30	9	18	21	3
		145.0	30	9	18	40	4
Cortisone	361.5	163.0	41	7	33	33	12
		121.0	41	7	33	47	15
		91.0	41	7	33	80	8

Table 1. Optimum conditions for the LC–MS/MS system. *DP* declustring potential, *EP* Entrance potential, *CEP* Collision cell entrance potential, *CE* Collision energy, *CXP* Collision cell exit potential.

calculated with respect to post-extraction spikes at the same nominal concentrations for both hydrocortisone and cortisone.

Results and discussion

LC–MS/MS optimizations

Mass-spectrometric conditions were established first by direct manual infusion of standard solutions in MeOH, followed by product-ion scans to identify intense and structurally informative fragments. For hydrocortisone, the protonated ion at m/z of 363.6 and its product ions at m/z of 121.0, 145.0 and 327.0 were monitored; the transition 363.6→121.0 was used for quantitative analysis, and 363.6→145.0 and 363.6→327.0 were used as qualifier transitions. For cortisone, the protonated ion at m/z of 361.5 and its product ions at m/z of 163.0, 121.0 and 91.0 were monitored; the transition 361.5→163.0 was used for quantitative analysis, with 361.5→121.0 and 361.5→91.0 serving as qualifier transitions. The declustering and entrance potentials, collision-cell parameters, and collision energies were iteratively adjusted by monitoring the product-ion spectra. Final settings were selected on the basis of maximal precursor to product response, stable qualifier-to-quantifier ratios, and absence of in-source artifacts. Multiple reaction monitoring (MRM) transitions were then verified under chromatographic elution to confirm retention-time alignment and ion-ratio conformity across concentrations. The optimized transitions and potentials are summarized in Table 1.

After the MS/MS parameters for the analytes were optimized, chromatographic variables were adjusted to secure baseline separation of the near-isomeric pair, preserve qualifier-to-quantifier ion-ratio conformity, and maintain a high signal-to-noise ratio within a short analysis cycle. Firstly, 6 reversed-phase columns (supplementary Table S2) were screened for optimized selectivity and efficiency. Among them, a Phenomenex

Gemini C18 analytical column provided a sufficient peak resolution for the analytes and was selected to be used for chromatographic separation.

Isocratic trials at intermediate organic contents yielded either partial co-elution or broadened, matrix-sensitive peaks. A stepwise gradient was therefore implemented to modulate elution strength over time, enhance differential retention between hydrocortisone and cortisone within a controlled window, and permit rapid re-equilibration. Ultrapure water with 0.10% formic acid was used as the mobile phase A and methanol with 0.10% formic acid as the mobile phase B. The gradient started at 70% A/30% B and was held to 2.0 min, followed by a change to 30% A/70% B between 2.0 and 5.0 min; this composition was maintained until 8.5 min, after which the system was returned to 70% A/30% B by 9.0 min and re-equilibrated at the initial conditions until 12.0 min. This program produced sharp, baseline-resolved peaks with stable retention times across runs, and the corresponding gradient profile is shown in supplementary Figure S1.

Temperature was investigated as solvent viscosity, diffusion coefficients, and stationary-phase selectivity are temperature dependent and directly influence peak resolution. Setpoints of 25, 45, and 60 °C were compared to find efficient condition. The chromatograms in supplementary Figure S2 show that increasing temperature compressed retention but reduced resolution between hydrocortisone and cortisone. The loss in resolution is consistent with diminished enthalpic contribution to selectivity at elevated temperature together with lower viscosity that reduces retention and narrows the available separation window[30]. At 25 °C, peaks remained narrow and symmetric, the baseline was stable, and the pair was fully resolved. A column temperature of 25 °C was therefore applied in subsequent work.

To avoid disruption of on-column focusing and degradation of peak shape by excessive loading or a strong-solvent plug, injection volume was optimized next. Volumes were examined across a practical range, and the responses are summarized in supplementary Figure S3. Peak area increased proportionally up to 25 µL with preserved symmetry, which indicates operation within the linear capacity of the stationary phase and adequate solvent-strength matching to the initial mobile phase. At volumes above 25 µL, fronting and peak asymmetry developed and resolution deteriorated, consistent with transient overload and partial breakthrough during the focusing step. An injection volume of 25 µL was therefore selected to maximize sensitivity while preserving chromatographic integrity.

Mobile-phase flow rate was then tuned to balance efficiency, resolution, and run time. Flow rates of 0.40, 0.50, 0.60, and 0.70 mL·min^{-1} were compared. As shown in supplementary Figure S4, increasing the flow from 0.40 to 0.60 mL min^{-1} decreased diffusion-dominated broadening and reduced tailing, while the pair remained fully resolved and the cycle time shortened. Further increase to 0.70 mL·min^{-1} did not improve signal-to-noise and marginally compressed the separation window. A flow rate of 0.60 mL·min^{-1} was therefore adopted because it afforded the shortest analysis time that maintained resolution at a satisfactory level and kept system backpressure within limits.

Under the combination of the final gradient, 25 °C column temperature, 25 µL injection volume, and 0.60 mL min^{-1} flow rate, retention times were stable, peaks were compact and symmetric, and qualifier-to-quantifier ion ratios met identification criteria in both artificial saliva matrices. Representative MRM chromatograms recorded under these conditions are provided in Fig. 2.

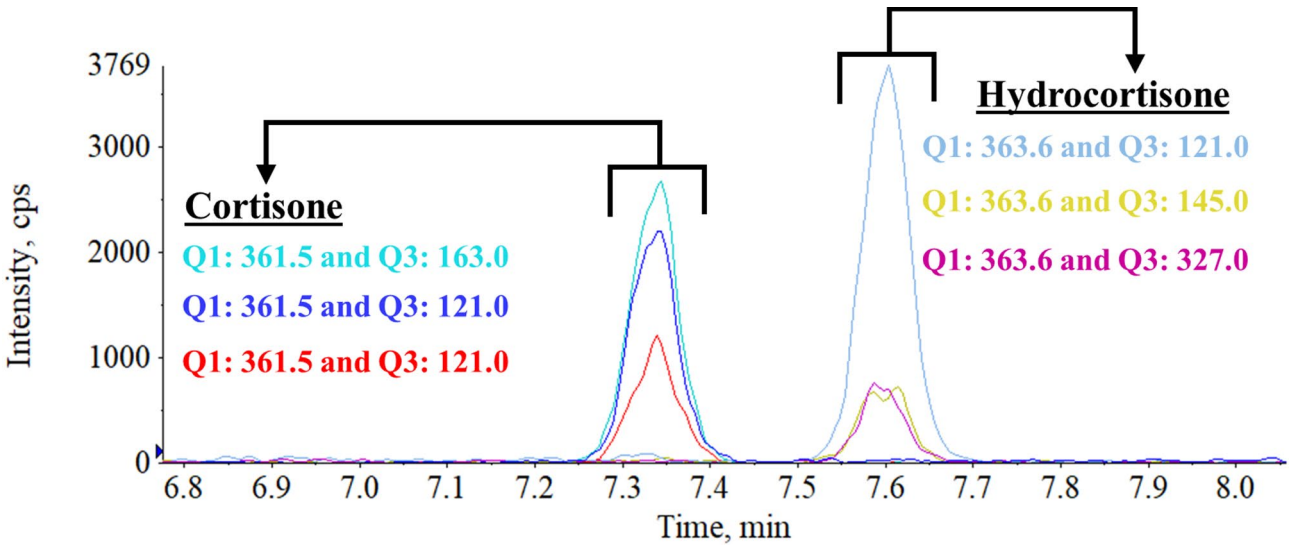

Fig. 2. MRM chromatograms monitored from a mix standard solution (Cortisone: 150.77 µg·kg^{-1} and Hydrocortisone: 107.05 µg·kg^{-1}).

Results of one-factor at a time optimization

A one-factor-at-a-time design was used to establish operating conditions for the SA-FDF-LPME before the LC–MS/MS analysis. Each parameter was varied independently while the others were held at provisional settings so that responses could be attributed to the single factor under study. The parameters included extraction solvent type, sample volume, spraying cycle, mixing period, eluent volume and eluent mixing period. The methanol fraction in the conditioned sample was kept constant to control solvent strength and isolate factor effects.

Variables were probed by peak area, signal-to-noise ratio, apparent enrichment factor and chromatographic integrity with attention to peak symmetry and the resolution of hydrocortisone from cortisone. Each condition was measured in triplicate, and matrix blanks were analyzed alongside to monitor background and carryover.

SA-FDF-LPME optimizations

At the beginning of the optimization studies regarding the microextraction procedure, the selection of the extraction solvent was prioritized. The solvent identity dictates the distribution coefficients for the steroids, the rheology of the atomized droplets, the kinetics of coalescence, and the ease of solvent removal at low temperatures[29,31,32]. Chloroform, 1,2-dichloroethane, and dichloromethane were investigated under identical conditions. Dichloromethane yielded the highest and most reproducible responses (Figure S5d, A). The outcome is consistent with strong solvation of moderately polar steroids, low viscosity that promotes formation of a fine aerosol, high density that forms a distinct lower layer with rapid phase disengagement, and sufficient volatility for gentle evaporation at 30 °C. Rapid separation limits re-equilibration losses and enables quantitative transfer of the organic phase.

After establishing the extractant, sample volume was addressed since liquid depth influences the phase ratio and the probability of productive microdroplet-analyte encounters[31,33]. Sample volumes of 6.0, 8.0, 10, and 12 mL were investigated. Signal intensity increased from 6.0 to 8.0 mL and then reached a plateau at higher volumes (Figure S5, B). The increase to 8.0 mL indicates more effective interception of the spray plume and an adequate interfacial area to drive mass transfer, whereas a deeper column disperses the droplet field without any added useful contact. A starting volume of 8.0 mL was therefore selected as the onset of the plateau with low variability.

With matrix volume fixed, attention turned to the spraying cycle, since extractant dose governs the attainable enrichment during the transient dispersion[29]. Two, three, and four spray cycles were compared to reach the highest signal-to-noise ratio for the analytes. Response increased from two to three cycles, consistent with a larger extractant volume and greater cumulative interfacial area (Figure S5, C). In addition, four spraying cycles did not provide a meaningful increase in signal intensity and resulted in a higher standard deviation compared to three cycles. This issue can be explained by the concept of diminishing returns, where additional solvent dilutes the collected organic phase and prolongs coalescence between the organic phase and the analytes without improving dispersion of the extraction solvent. Therefore, three cycles were adopted as the working condition.

Hydrodynamic assistance immediately after the spraying cycle was also investigated, as brief mixing can accelerate mass transfer, but prolonged contact can promote back-extraction[29]. Measurable extraction was observed even without mixing, which reflects the micro dispersion generated by the spray, yet responses were low and variable. Introducing 15 s of mixing increased the signal-to-noise ratio and improved repeatability by promoting rapid droplet-bulk contact and clean coalescence (Figure S5, D). Extending the period to 30, 45, and 60 s produced a progressive decline, which can be attributed to the release of the analytes from the organic phase back into the aqueous phase. A brief 15-second mix preserves the kinetically captured enrichment and limits re-equilibration.

Finally, post-extraction handling was optimized to secure complete dissolution without unnecessary dilution. After full removal of the dichloromethane layer in a vacuum oven at 30 °C, the residue was reconstituted with methanol at volumes of 50, 75, 100, and 125 µL. A volume of 50 µL methanol achieved complete dissolution and produced the highest responses with symmetric peaks (Figure S5, E). Larger volumes did not improve dissolution and they lowered the signal in proportion with the corresponding dilution factors[34]. Eluent mixing periods of 10, 20, and 30 s gave indistinguishable outcomes (Figure S5, F), indicating that homogeneity was reached at the shortest period, so a mixing for 10 s after the addition of methanol was utilized to maintain consistency while minimizing the handling period.

These studies identified dichloromethane as the extractant, established 8.0 mL as the working sample volume, supported three spray actuations, recommended 15 s of post-spray mixing, and defined 50 µL as the eluent volume with a 10-second eluent mixing period. Together, these conditions were shown to maximize response and preserve chromatographic symmetry and retention-time stability.

Analytical figures of merit of LC–MS/MS and SA-FDF-LPME-LC–MS/MS

Under the optimized LC–MS/MS conditions, standard solutions in methanol were injected to characterize the system performance for both analytes. For cortisone, a six-point calibration line defined a dynamic working range (LDR) of 3.65–150.77 µg kg^{-1}, and a nine-point calibration curve covered 3.65–1497.3 µg kg^{-1}, with the LOD and LOQ at 1.05 µg $kg^{-1}$and 3.50 µg kg^{-1}, respectively. For hydrocortisone, a seven-point calibration line established a dynamic range of 2.59–268.45 µg kg^{-1}, and a nine-point calibration curve spanned 2.59–1063.1 µg kg^{-1}, with the LOD and LOQ at 0.80 µg kg^{-1} and 2.68 µg kg^{-1}. Multiple reaction monitoring was used

throughout with stable retention and ion-ratio conformity, linear response was supported by the calibration fits. Representative calibration plots, complete calibration curves, and LOQ chromatograms are provided in supplementary Figure S6.

Performance of the sample preparation approach was established by subjecting aqueous calibration standards to the SA-FDF-LPME and analyzing the resulting extracts by the LC–MS/MS, from which the dynamic working range and detection capability were derived. For cortisone, the dynamic working range was recorded as 0.050–4.98 µg kg^{-1} with a seven-point calibration plot, and the calibration curve covered 0.050–102.92 µg kg^{-1}. The LOD and LOQ were recorded as 16.41 ng $kg^{-1}$and 54.70 ng kg^{-1}, respectively. For hydrocortisone, the dynamic working range was recorded as 0.21–5.50 µg kg^{-1} with a five-point calibration plot, and the calibration curve covered 0.21–201.65 µg kg^{-1}. The LOD and LOQ were recorded as 73.38 ng $kg^{-1}$and 244.61 ng kg^{-1}, respectively. Representative calibration plots and LOQ chromatograms obtained after the SA-FDF-LPME are presented in Fig. 3, and consolidated figures of merit for both systems are summarized in Table 2.

In a comparative evaluation of direct-injection LC–MS/MS versus SA-FDF-LPME coupled to LC–MS/MS, clear gains in sensitivity were observed. The enhancement in detection power (EDP) was 64.0-fold for cortisone and 11.0-fold for hydrocortisone, and the enhancement in calibration sensitivity (ECS) reached 68.6-fold for cortisone and 14.8-fold for hydrocortisone. LOD, LOQ, EDP, and ECS were calculated using the standard expressions provided below.

$$LOD = 3 \bullet \frac{Standard\ deviation\ of\ the\ lowest\ concnetration\ found\ in\ calibration\ plot}{Slope\ of\ calibration\ plot} \quad (1)$$

$$LOQ = 10 \bullet \frac{Standard\ deviation\ of\ the\ lowest\ concnetration\ found\ in\ calibration\ plot}{Slope\ of\ calibration\ plot} \quad (2)$$

$$The\ enhancement\ in\ quantitation\ power\ of\ LC?MS/MS\ system = \frac{LOQ\ value\ of\ \mathrm{SA-FDF-LPME-LC-MS/MS}\ method}{LOQ\ value\ of\ \mathrm{LC-MS/MS}\ system} \quad (3)$$

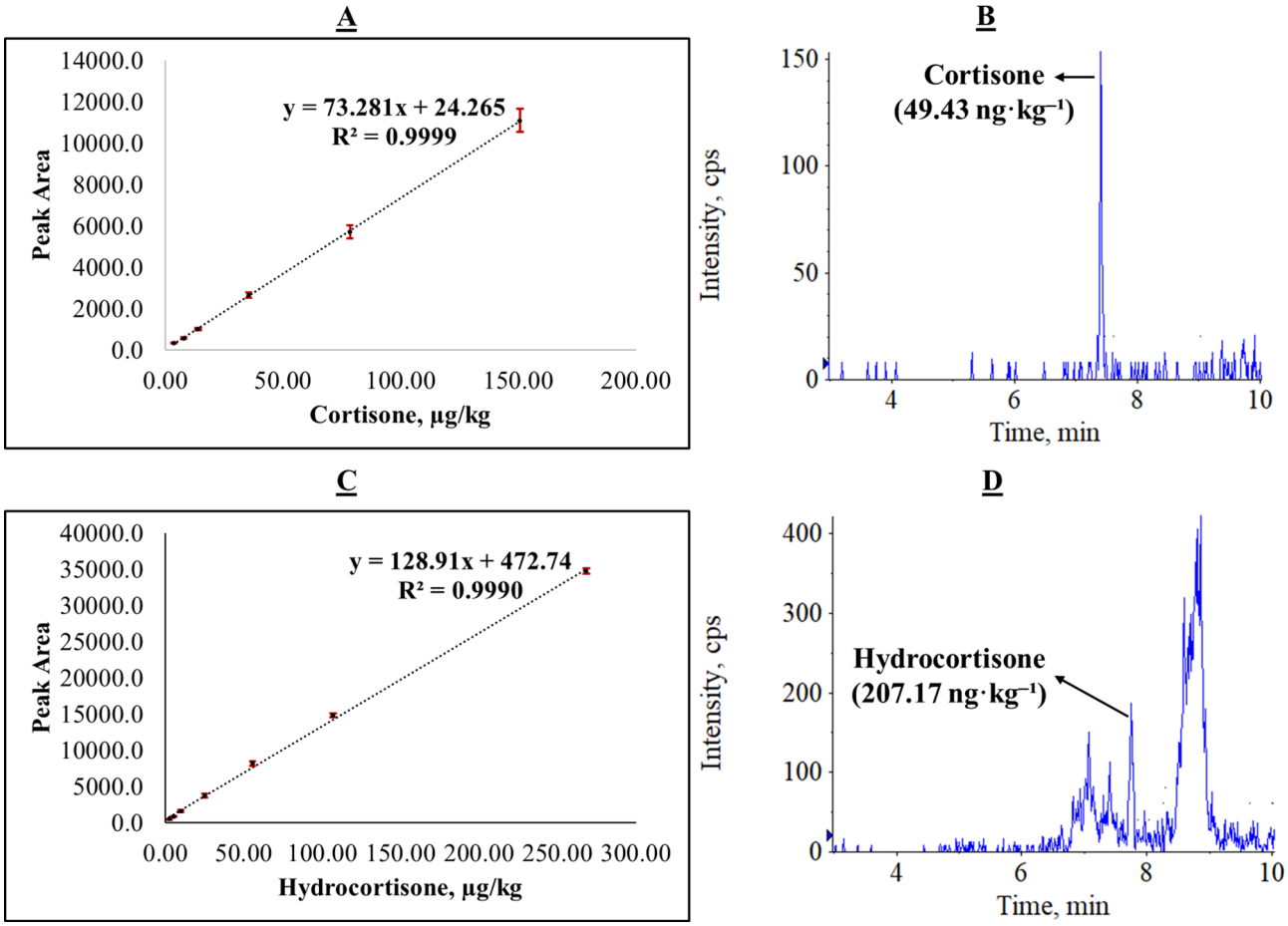

Fig. 3. Calibration plot (**A**) and LOQ signal (**B**) obtained from the SA-FDF-LPME-LC–MS/MS method for cortisone and calibration plot (**C**) and LOQ signal (**D**) obtained from the SA-FDF-LPME-LC–MS/MS method for hydrocortisone.

Analyte	Method	LOD[a]	LOQ[b]	Dynamic range	EDP[c]	ECS[d]	Reference
Cortisone	LC–MS/MS[e]	1.05 μg·kg^{-1}	3.50 μg·kg^{-1}	3.65 μg·kg^{-1}–150.77 μg·kg^{-1}	–	–	Current study
	SA-FDF-LPME-LC–MS/MS[f]	16.41 ng·kg^{-1}	54.70 ng·kg^{-1}	49.43 ng·kg^{-1}–4.98 μg·kg^{-1}	64.0	68.6	
Hydrocortisone	LC–MS/MS[e]	0.80 μg·kg^{-1}	2.68 μg·kg^{-1}	2.59 μg·kg^{-1}– 268.45 μg·kg^{-1}	–	–	
	SA-FDF-LPME-LC–MS/MS[f]	73.38 ng·kg^{-1}	244.61 ng·kg^{-1}	207.17 ng·kg^{-1}–5.50 μg·kg^{-1}	11.0	14.8	
Cortisone	LC–MS/MS[e]	1.0 μg·L^{-1}	2.5 μg/L μg·L^{-1}	2.5–100 μg·L^{-1}	–	–	35
Cortisol (hydrocortisone)		0.2 μg·L^{-1}	1.0 μg·L^{-1}	1.0–500 μg·L^{-1}	–	–	
Cortisone	LC–MS/MS[e]	2.0 μg·L^{-1}		2.5–300 μg·L^{-1}	–	–	36
Cortisol (hydrocortisone)					–	–	
Cortisone	LC–MS/MS[e]	0.56 nmol·L^{-1} (~ 0.20 μg·L^{-1})	–	–	–	–	37
Cortisol (hydrocortisone)		0.69 nmol·L^{-1} (~ 0.25 μg·L^{-1})	–	–	–	–	
Cortisone	LC–MS/MS[e]	0.43 μg·L^{-1}	1.0 μg·L^{-1} (LLOQ)[g]	1–150 μg·L^{-1}	–	–	38
Cortisol (hydrocortisone)		0.22 μg·L^{-1}	1.0 μg·L^{-1} (LLOQ)[g]	1–150 μg·L^{-1}	–	–	
Cortisone	LC–MS/MS[e]	0.3 nmol·L^{-1}	0.55 nmol·L^{-1} (0.20 μg·L^{-1}) (LLOQ)[g]	–	–	–	39
Cortisol (hydrocortisone)		0.2 nmol·L^{-1} (0.11 μg·L^{-1})	0.51 nmol·L^{-1} (0.18 μg·L^{-1}) (LLOQ)[g]	–	–	–	

Table 2. System analytical performance parameters of LC–MS/MS and SA-FDF-LPME-LC–MS/MS measurements along with comparable figures from literature. [a]LOD: Limit of detection. [b]LOQ: Limit of quantification. [c]EDP: Enhancement in detection power. [d]ECS: Enhancement in calibration sensitivity. [e]LC–MS/MS: Liquid chromatography–tandem mass spectrometry. [f]SA-FDF-LPME-LC–MS/MS: Spray assisted fine droplet formation liquid phase microextraction – liquid chromatography–tandem mass spectrometry. [g]LLOQ: Lower Limit of quantification.

$$The\ enhancement\ in\ calibration\ sensitivity\ of\ LC?MS/MS\ system = \frac{Slope\ of\ the\ \mathrm{SA-FDF-LPME-LC-MS/MS}\ method}{Slope\ of\ the\ \mathrm{LC-MS/MS}\ system} \quad (4)$$

When compared with representative LC–MS/MS methods reported in the literature, the SA-FDF-LPME-LC–MS/MS method delivered lower LOD/LOQ values and a practical dynamic working range. As shown in Table 2, both hydrocortisone and cortisone were quantified at concentrations below those typically reported in saliva[9,40], while maintaining ratio reliability and chromatographic resolution appropriate for saliva-level measurements. Although the scope of this investigation focuses on hydrocortisone and cortisone, the results suggest that the SA-FDF-LPME platform can be coupled to LC–MS/MS for other steroids and small molecules, where similar gains in sensitivity and robustness are anticipated.

Recovery experiments

The two representative matrices, artificial saliva A and B were prepared as described in Sect. 2.3, spiked before extraction at various concentration levels for each analyte, and processed in triplicate. Samples were extracted by following the proposed SA-FDF-LPME procedure and were chromatographed and quantified by the LC–MS/MS. Quantification was first carried out by the external standard calibration method, using already established calibration lines for back-calculation of the concentrations from the peak-area responses (supplementary Figure S7). This approach provided recoveries in the ranges of 105.3%–129.4% and 110.4%–141.1% for cortisone in the spiked artificial saliva A and B sample sets respectively. The recovery values for hydrocortisone in the spiked artificial saliva A and B sample sets were calculated as 110.0–134.9.0.9% and 94.1–142.8.1.8%. It is clear from the figures that the results for both analytes indicate remarkable matrix influence when water-based calibration is used.

To compensate for matrix-dependent effects, matrix-matched calibration standards were prepared separately for the spiked artificial saliva A and B matrices to be analyzed in the same manner to back-calculate concentrations (supplementary Figure S8). Recoveries then converged toward nominal values. Cortisone yielded recovery results ranging between 80.3% and 103.2% in the spiked artificial saliva A samples and 98.1%–117.8% in the spiked artificial saliva B samples. Hydrocortisone recoveries were recorded as 79.8%–105.7% in the spiked artificial saliva A and 97.3%–114.0% in the spiked artificial saliva B samples. The calibration line equations given in supplementary Figure S8 (A) and Figure S8 (B) were used to calculate the percent recovery results for cortisone in the spiked artificial saliva B and A samples, respectively. The same approach was also implemented to determine the percent recovery results for hydrocortisone using the matrix-matched calibration plots (supplementary Figure S8 (C) and Figure S8 (D)). Additionally, the improvement is consistent with the measured matrix effects, which were + 11.0% for cortisone in the artificial saliva A and + 11.5% in the artificial saliva B, and – 37.9% for hydrocortisone in the artificial saliva A and – 36.8% in the artificial saliva B. During the calculation of matrix effects, the formula " $\%Matrix\ effect = \frac{Slope\ of\ the\ related\ matrix-matched\ calibration\ plot}{Slope\ of\ the\ external\ standard\ calibration\ plot} - 1$" was employed. All

			External Standard Calibration		Matrix-matched Calibration	
Sample	Analyte	Spiked Concentration, µg·kg^{-1}	Recovery, %	±SD *	Recovery, %	±SD *
Artificial Saliva A	Cortisone	0.50	117.6	4.6	80.3	4.1
		0.98	129.4	3.1	103.2	2.8
		3.43	105.3	6.6	90.7	5.9
		5.43	114.4	10.4	100.3	9.4
Artificial Saliva B		0.49	141.1	17.2	117.8	15.5
		0.99	122.1	10.2	105.4	9.2
		1.60	128.3	7.4	112.7	6.7
		3.48	110.4	11.8	98.1	10.6
		5.32	115.8	9.5	103.5	8.6
Artificial Saliva A	Hydrocortisone	0.99	134.9	8.9	79.8	14.1
		1.93	110.0	7.8	105.7	12.4
		6.73	-	-	90.4	13.5
		10.64	-	-	99.3	3.7
Artificial Saliva B		0.95	142.8	14.1	101.9	22.7
		1.94	109.9	10.9	114.0	17.6
		3.13	94.1	6.9	112.5	11.1
		6.82	-	-	97.3	6.8
		10.42	-	-	104.7	1.7

Table 3. Percent recoveries for artificial saliva obtained with the SA-FDF-LPME-LC–MS/MS method using the external standard and matrix-matched calibration strategies. *SD: Standard deviation for $n = 3$.

recovery results for both calibration strategies are compiled in Table 3, and representative chromatograms of standards and spiked saliva extracts after the SA-FDF-LPME are presented in Fig. 4.

Conclusion

A simple and effective analytical method was developed for trace-level determination of hydrocortisone and cortisone in saliva-type matrices. To the best of current knowledge, this is the first study combining spraying assisted fine droplet formation liquid-phase microextraction (SA-FDF-LPME) with LC–MS/MS for the simultaneous determination of hydrocortisone and cortisone in artificial saliva matrices representative of saliva composition. The LC–MS/MS conditions were optimized for low detection limits and robust chromatography, and the SA-FDF-LPME variables were refined in parallel. Under direct injection, the LOD and LOQ values were calculated as 1.05 µg kg^{-1} and 3.50 µg kg^{-1} for cortisone and 0.80 µg kg^{-1} and 2.68 µg kg^{-1} for hydrocortisone. Furthermore, the dynamic working ranges for cortisone and hydrocortisone recorded via the LC–MS/MS system were 3.65–150.77 µg kg^{-1} and 2.59–268.45 µg kg^{-1}, respectively. With the SA-FDF-LPME coupled to the LC–MS/MS, the LOD and LOQ values were calculated as 16.41 ng kg^{-1} and 54.70 ng kg^{-1} (with a dynamic working range of 49.43 ng·kg^{-1}–4.98 µg·kg^{-1}) for cortisone and 73.38 ng kg^{-1} and 244.61 ng kg^{-1} (with a dynamic working range of 207.17 ng kg^{-1}–5.50 µg kg^{-1}) for hydrocortisone. Sensitivity gains were quantified as EDP 64.0-fold for cortisone and 11.0-fold for hydrocortisone. In addition, the calibration sensitivity of the LC–MS/MS system was augmented 68.6-fold and 14.8-fold for cortisone and hydrocortisone after the implementation of the SA-FDF-LPME method. Accuracy in two artificial saliva formulations was demonstrated by pre-extraction spiking at several concentration levels for each analyte, where the external standard calibration resulted in recoveries of 105.3%–141.1% for cortisone and 94.1%–142.8% for hydrocortisone, and matrix-matched calibration yielded 80.3%–117.8% for cortisone and 79.8%–114.0% for hydrocortisone. The findings indicate that the developed SA-FDF-LPME-LC–MS/MS method is suitable for the qualitative and quantitative determination of hydrocortisone and cortisone in artificial saliva matrices at trace concentrations with demonstrated accuracy and repeatability. Building on the analytical performance demonstrated in saliva-type matrices, extension of the proposed approach to native human saliva for clinical quantification can be addressed in future studies following established bioanalytical frameworks such as ICH M10. Moreover, the SA-FDF-LPME strategy is readily applicable in combination with a LC–MS/MS system to other non-volatile, poorly water-soluble steroids and small-molecule analytes where low detection limits and ratio-reliable quantification are required.

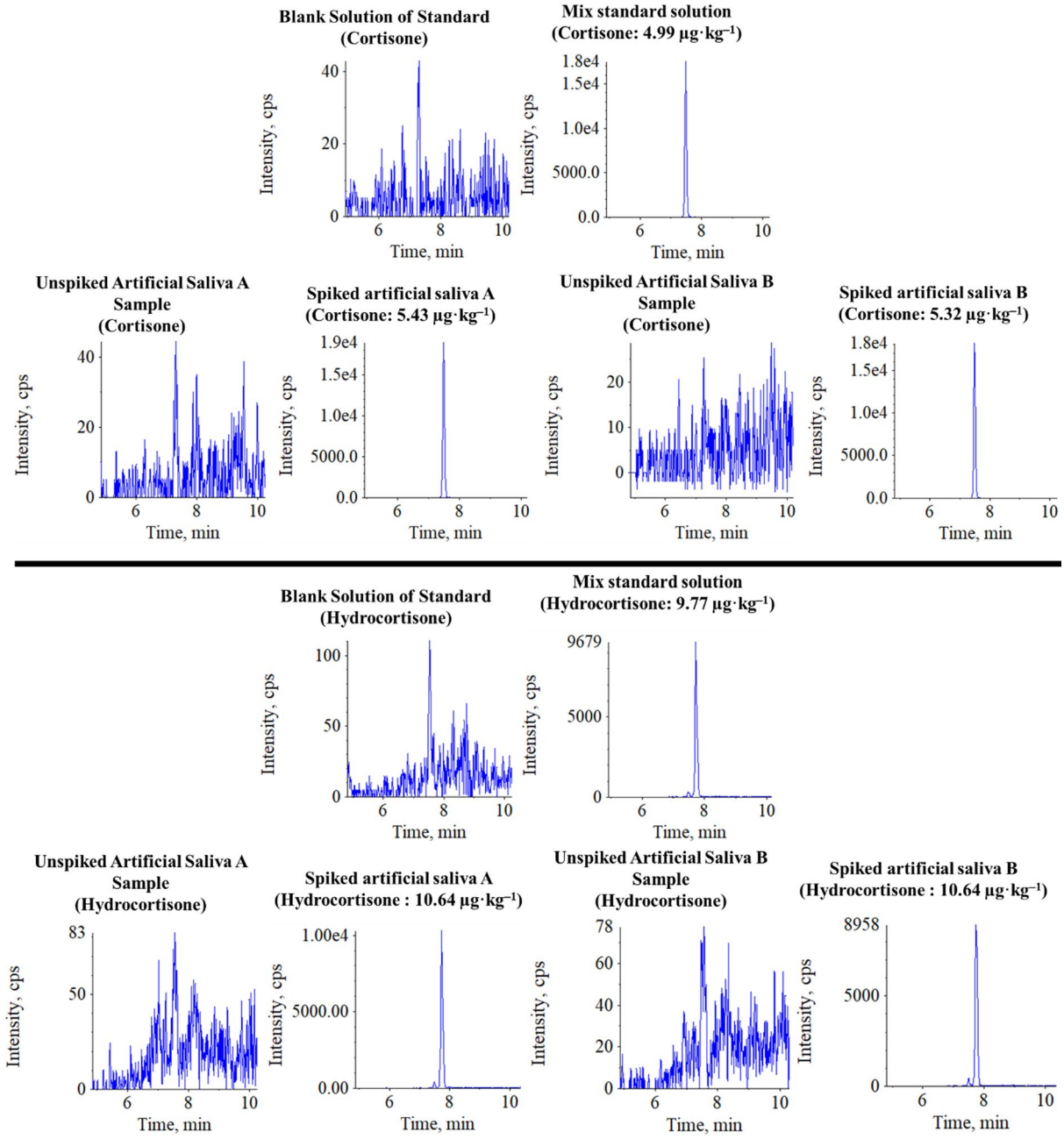

Fig. 4. Representative MRM chromatograms recorded from the standard/blank solutions and unspiked/spiked samples acquired following the SA-FDF-LPME-LC–MS/MS method.

Data availability

Data will be made available on reasonable request. Kindly contact with the corresponding author.

Received: 7 November 2025; Accepted: 29 January 2026
Published online: 03 February 2026

References

1. Akalestou, E., Genser, L. & Rutter, G. A. Glucocorticoid metabolism in obesity and following weight loss. *Front. Endocrinol. (Lausanne)*. **11**, 509361 (2020).
2. Oster, H. et al. The functional and clinical significance of the 24-hour rhythm of circulating glucocorticoids. *Endocr. Rev.* **38**, 3–45 (2017).
3. Quinkler, M. & Stewart, P. M. Hypertension and the cortisol-cortisone shuttle. *J. Clin. Endocrinol. Metab.* **88**, 2384–2392 (2003).
4. Draper, N. & Stewart, P. M. 11beta-hydroxysteroid dehydrogenase and the pre-receptor regulation of corticosteroid hormone action. *J. Endocrinol.* **186**, 251–271 (2005).

5. Stimson, R. H. et al. Cortisol release from adipose tissue by 11beta-hydroxysteroid dehydrogenase type 1 in humans. *Diabetes* **58**, 46–53 (2009).
6. Rabbitt, E. H. et al. Prereceptor regulation of glucocorticoid action by 11beta-hydroxysteroid dehydrogenase: a novel determinant of cell proliferation. *FASEB J.* **16**, 36–44 (2002).
7. Funder, J. W. Apparent mineralocorticoid excess. *J. Steroid Biochem. Mol. Biol.* **165**, 151–153 (2017).
8. Vuppaladhadiam, L. et al. Human placenta buffers the fetus from adverse effects of perceived maternal stress. *Cells* **10**, 379 (2021).
9. Jung, C. et al. Plasma, salivary and urinary cortisol levels following physiological and stress doses of hydrocortisone in normal volunteers. *BMC Endocr. Disord.* **14**, 1–10 (2014).
10. Hardy, R. S. et al. 11βHSD1 Inhibition with AZD4017 improves lipid profiles and lean muscle mass in idiopathic intracranial hypertension. *J. Clin. Endocrinol. Metab.* **106**, 174 (2020).
11. Bailey, M. A. 11β-Hydroxysteroid dehydrogenases and hypertension in the metabolic syndrome. *Curr. Hypertens. Rep.* **19**, 100 (2017).
12. El-Farhan, N., Rees, D. A. & Evans, C. Measuring cortisol in serum, urine and saliva: are our assays good enough?. *Ann. Clin. Biochem.* **54**, 308–322 (2017).
13. Gröschl, M. Current status of salivary hormone analysis. *Clin. Chem.* **54**, 1759–1769 (2008).
14. Xia, Y. Q. & Jemal, M. Phospholipids in liquid chromatography/mass spectrometry bioanalysis: comparison of three tandem mass spectrometric techniques for monitoring plasma phospholipids, the effect of mobile phase composition on phospholipids elution and the association of phospholipids with matrix effects. *Rapid Commun. Mass. Spectrom.* **23**, 2125–2138 (2009).
15. Ponzetto, F. et al. Reference ranges of late-night salivary cortisol and cortisone measured by LC–MS/MS and accuracy for the diagnosis of cushing's syndrome. *J. Endocrinol. Invest.* **43**, 1797–1806 (2020).
16. Sharma, V. V. & Lanekoff, I. Revealing structure and localization of steroid regioisomers through predictive fragmentation patterns in mass spectrometry imaging. *Anal. Chem.* **95**, 17843–17850 (2023).
17. Ionita, I. A., Fast, D. M. & Akhlaghi, F. Development of a sensitive and selective method for the quantitative analysis of cortisol, cortisone, prednisolone and prednisone in human plasma. *J. Chromatogr. B Analyt Technol. Biomed. Life Sci.* **877**, 765–772 (2009).
18. Casals, G. et al. LC-HRMS and GC-MS profiling of urine free cortisol, cortisone, 6B-, and 18-hydroxycortisol for the evaluation of glucocorticoid and mineralocorticoid disorders. *Biomolecules* **14**, 558 (2024).
19. Monaghan, P. J. et al. Comparison of serum cortisol measurement by immunoassay and liquid chromatography-tandem mass spectrometry in patients receiving the 11β-hydroxylase inhibitor Metyrapone. *Ann. Clin. Biochem.* **48**, 441–446 (2011).
20. Amendola, L., Garribba, F. & Botrè, F. Determination of endogenous and synthetic glucocorticoids in human urine by gas chromatography–mass spectrometry following microwave-assisted derivatization. *Anal. Chim. Acta*. **489**, 233–243 (2003).
21. Allende, F. et al. LC–MS/MS method for the simultaneous determination of free urinary steroids. *Chromatographia* **77**, 637–642 (2014).
22. Ponzetto, F. et al. Simultaneous measurement of cortisol, cortisone, dexamethasone and additional exogenous corticosteroids by rapid and sensitive LC–MS/MS analysis. *Molecules* **28**, 248 (2023).
23. Yamini, Y., Rezazadeh, M. & Seidi, S. Liquid-phase microextraction: The different principles and configurations. *TRAC Trends Anal. Chem.* **112**, 264–272 (2019).
24. Kokosa, J. M. Recent trends in using single-drop microextraction and related techniques in green analytical methods. *TRAC Trends Anal. Chem.* **71**, 194–204 (2015).
25. Bodur, S., Erarpat, S., Tutar, Ö. F. & Bakırdere, S. A simple spray assisted extraction/preconcentration of cadmium from sunflower oil, olive oil and hazelnut oil samples prior to flame atomic absorption spectrometry determination. *J. Food Compos. Anal.* **117**, 105144 (2023).
26. Voidarou, C. et al. An in vitro study of different types of Greek honey as potential natural antimicrobials against dental caries and other oral pathogenic microorganisms: Case study simulation of oral cavity conditions. *Appl. Sci. 2021* **11**, 6318 (2021).
27. Pietrzyńska, M. & Voelkel, A. Stability of simulated body fluids such as blood plasma, artificial urine and artificial saliva. *Microchem. J.* **134**, 197–201 (2017).
28. Öztürk Er, E., Özbek, B. & Bakırdere, S. Determination of seventeen free amino acids in human urine and plasma samples using quadruple isotope dilution mass spectrometry combined with hydrophilic interaction liquid chromatography–Tandem mass spectrometry. *J. Chromatogr. A* **1641**, 461970 (2021).
29. Dikmen, Y. et al. A novel and rapid extraction protocol for sensitive and accurate determination of Prochloraz in orange juice samples: Vortex-assisted spraying-based fine droplet formation liquid-phase Microextraction before gas chromatography-mass spectrometry. *J Mass. Spectrom* **55,** e4622 (1-7), (2020).
30. Chen, L. C. High-Temperature liquid chromatography and the hyphenation with mass spectrometry using high-pressure electrospray ionization. *Mass. Spectrom.* **8**, S0079 (2019).
31. Zaruba, S., Ovšonková, M., Makoś-Chełstowska, P. & Andruch, V. A closer look at how the dispersive liquid–liquid microextraction method works: Investigation of the effect of solvent mixture composition on the quality and stability of the cloudy state. *Front. Chem.* **12**, 1383445 (2024).
32. Urge, A. Y., Pampanin, D. M., Martino, M. E., Knudsen, D. L. & Brede, C. Salting-out assisted liquid–liquid extraction for UPLC–MS/MS determination of thyroxine and steroid hormones in human serum and fish plasma. *Sep. 2023* **10, Page 240**(10), 240 (2023).
33. Yu, S., Zhang, J., Li, S., Chen, Z. & Wang, Y. Mass transfer and droplet behaviors in liquid–liquid extraction process based on multi-scale perspective: A review. *Sep. 2023* **10, Page 264**(10), 264 (2023).
34. Gürsoy, S. et al. Determination of Ethalfluralin in soy flour samples using MnO2-deep eutectic solvent based nanofluid for its preconcentration prior to GC-FID measurement. *Chem. Pap.* **78**, 6545–6552 (2024).
35. Lee, S. et al. Simultaneous determination of cortisol and cortisone from human serum by liquid chromatography–tandem mass spectrometry. *J Anal Methods Chem* **2014**, 787483 (2014).
36. Taylor, R. L., Machacek, D. & Singh, R. J. Validation of a high-throughput liquid chromatography–tandem mass spectrometry method for urinary cortisol and cortisone. *Clin. Chem.* **48**, 1511–1519 (2002).
37. Kunz, S. et al. Fast and reliable quantification of aldosterone, cortisol and cortisone via LC–MS/MS to study 11β-hydroxysteroid dehydrogenase activities in primary cell cultures. *J. Steroid Biochem. Mol. Biol.* **244**, 106610 (2024).
38. Leoni, L. et al. Determination of human urinary cortisol, cortisone and relative phase II metabolites by dilute-and-shoot LC–MS/MS analysis: an application to adrenal disease. *Clin. Chim. Acta*. **574**, 120324 (2025).
39. Antonelli, G., Ceccato, F., Artusi, C., Marinova, M. & Plebani, M. Salivary cortisol and cortisone by LC–MS/MS: validation, reference intervals and diagnostic accuracy in cushing's syndrome. *Clin. Chim. Acta*. **451**, 247–251 (2015).
40. Debono, M. et al. Salivary cortisone reflects cortisol exposure under physiological conditions and after hydrocortisone. *J. Clin. Endocrinol. Metab.* **101**, 1469–1477 (2016).

Author contributions

Selim Gürsoy: Formal analysis; Investigation; Methodology; Validation; Visualization; Roles/Writing - original draft. Süleyman Bodur: Data curation, Formal analysis; Methodology; Validation; Roles/Writing - original draft. Arda Atakol: Formal analysis; Methodology; Validation; Roles/Writing - original draft. Sezgin Bakırdere: Conceptualization; Investigation; Methodology; Supervision; Validation; Writing - review & editing.

Funding
None.

Declarations

Competing interests
The authors declare no competing interests.

Ethical approval
This article does not contain any studies with human participants or animals performed by any of the authors.

Additional information
Supplementary Information The online version contains supplementary material available at https://doi.org/10.1038/s41598-026-38457-z.

Correspondence and requests for materials should be addressed to S.B.

Reprints and permissions information is available at www.nature.com/reprints.

Publisher's note Springer Nature remains neutral with regard to jurisdictional claims in published maps and institutional affiliations.